MIT Libraries | DSpace@MIT

MIT Open Access Articles

In-Plane Ferroelectric Tunnel Junction

The MIT Faculty has made this article openly available. ***Please share*** how this access benefits you. Your story matters.

Citation: Shen, Huitao et al. "In-Plane Ferroelectric Tunnel Junction." Physical Review Applied 11 (2019): 024048 © 2019 The Author(s)

As Published: http://dx.doi.org/10.1103/PhysRevApplied.11.024048

Publisher: American Physical Society

Persistent URL: https://hdl.handle.net/1721.1/125318

Version: Final published version: final published article, as it appeared in a journal, conference proceedings, or other formally published context

Terms of Use: Article is made available in accordance with the publisher's policy and may be subject to US copyright law. Please refer to the publisher's site for terms of use.

Massachusetts Institute of Technology

Editors' Suggestion

In-Plane Ferroelectric Tunnel Junction

Huitao Shen,[1,*] Junwei Liu,[2] Kai Chang,[3] and Liang Fu[1]

[1] *Department of Physics, Massachusetts Institute of Technology, Cambridge, Massachusetts 02139, USA*
[2] *Department of Physics, Hong Kong University of Science and Technology, Clear Water Bay, Hong Kong, China*
[3] *Max Planck Institute of Microstructure Physics, Weinberg 2, 06120 Halle (Saale), Germany*

(Received 24 July 2018; revised manuscript received 13 December 2018; published 20 February 2019)

Ferroelectric materals are an important platform for the realization of nonvolatile memories. So far, existing ferroelectric memory devices have utilized out-of-plane polarization in ferroelectric thin films. In this paper, we propose a type of random-access memory (RAM) based on ferroelectric thin films with in-plane polarization, called an "in-plane ferroelectric tunnel junction." Apart from nonvolatility, lower power usage, and a faster writing operation compared with traditional dynamic RAMs, our proposal has the advantage of a faster reading operation and a nondestructive reading process, thus overcoming the write-after-read problem that exists widely in current ferroelectric RAMs. The recent discovered room-temperature ferroelectric IV-VI semiconductor thin films are a promising material platform for the realization of our proposal.

DOI: 10.1103/PhysRevApplied.11.024048

I. INTRODUCTION

To meet the daily increasing demands of modern electronic devices, especially those of portable devices, memories with a low energy consumption and high performance are highly desirable. The current commercial dynamic random-access memories (DRAMs) are volatile and consume a large amount of energy to refresh the stored data in order to prevent leakage from the capacitor. To reduce the energy consumption, a nonvolatile memory might be the ultimate solution [1,2].

Ferroelectric materials have been proposed as ideal candidates for nonvolatile memories due to their electric switchable bistable ground states since 1952 [3] and ferroelectricity-based nonvolatile memories have been developed rapidly over recent decades [4,5].

Depending on the readout mechanism, ferroelectric nonvolatile memories can be roughly classified into two generations. The first generation of ferroelectric RAM (FERAM) uses polarized charges in the ferroelectric capacitor to represent the data [6–8]. As a result, discharging the capacitor to measure the polarized charge destroys the stored data and the capacitor needs to be recharged after the reading operation. Limited by the destructive reading process, the ferroelectric size effects [9,10], and various practical issues such as fatigue [11] and imprint [12], the market for FERAMs remains relatively small.

To overcome the destructive readout problem, a second generation of ferroelectric tunnel junctions (FTJs) has been proposed to probe the ferroelectric polarization using the tunneling-electroresistance effect [13–15]. The basic structure of the FTJ is a metal-ferroelectric-metal junction, where the tunneling potential barrier is determined by the out-of-plane polarization in the ferroelectric layer. In this way, the FTJ realizes bistable resistance states. The major challenge of realizing an FTJ is to fabricate ultrathin ferroelectric films so that the tunneling current surpasses the threshold of the peripheral amplifiers. The depolarization field induced by the out-of-plane polarization dramatically suppresses the ferroelectric critical temperature or even destroys the ferroelectricity when the films are too thin [16–19].

In this work, we propose a type of ferroelectric memory that we call an "in-plane ferroelectric tunnel junction." Unlike FERAMs or FTJs, which employ bistable states of out-of-plane ferroelectric polarization to represent "on" and "off", our proposal is based on the in-plane polarization of ferroelectric thin films. Due to the insufficient screening in two dimensions, the in-plane polarization could induce strong band bending around an interface such as the material edge or the ferroelectric-domain wall. Depending on the polarization direction, the upward or downward band bending could be used to represent the on or off state respectively. By measuring the out-of-plane tunneling current through ferroelectric thin films, the bending direction can be detected and hence the stored information can be read nondestructively. Moreover, our design enjoys great tunability. By choosing proper layer sizes and the insulator-layer band gap, the tunneling current and the on:off current ratio can be tuned simultaneously. In principle, all ferroelectric thin films with in-plane polarization can be used as the material platform to realize our

*huitao@mit.edu

 © 2019 American Physical Society

proposal [20–30]. In particular, the recently discovered room-temperature IV-VI semiconductor thin films with robust in-plane polarization are ideal candidates [25,26].

The paper is organized as follows. We first introduce in-plane ferroelectric polarizations and the induced robust band bending. We then demonstrate the device design and explain its reading and writing mechanism in detail. The demonstration is supported by the quantum-mechanical tunneling-current simulation. Finally, we discuss the advantage of our design over conventional ferroelectricity-based memories.

II. IN-PLANE POLARIZATION

Ferroelectricity as a symmetry-breaking state is generally destabilized by the finite-size effect. The out-of-plane ferroelectric polarization is found in perovskite ultrathin films, in which imperfect charge screening, substrate strain, and chemical bonding play important roles in stabilizing the ferroelectricity [31–36]. As already mentioned in Sec. I, the critical temperature of these perovskite ferroelectric materials decreases with the film thickness. On the other hand, in-plane polarization in perovskite thin films [20–23] and even liquid crystals [24] has been studied. Although it is predicted that in-plane polarization will survive in the two-dimensional (2D) limit [19], it is currently hard to prepare free-standing 2D perovskite ferroelectrics.

Surprisingly, the recently discovered in-plane polarization in 2D ferroelectrics is enhanced instead of reduced in thin films [25,27–30]. For example, in SnTe, compared with the bulk-ferroelectric transition temperature of 98 K, the one-monolayer (ML) thin film has a critical temperature of 270 K, and thicker 3-ML films show robust spontaneous polarization even at room temperature [25,26]. Moreover, the weak van der Waals interlayer coupling enables more freedom in device design as, in principle, 2D materials can be stacked freely without the constraint of lattice mismatching.

An important signature of in-plane polarization is the band bending near an interface such as the material edge [25] or the ferroelectric-domain wall [37]. Taking the material edge as an example, without screening, the bound charges induced by the in-plane ferroelectric polarization $\sigma_b = \mathbf{P} \cdot \mathbf{n}$ are of opposite signs at the two boundaries, where $\mathbf{P}$ is the polarization vector and $\mathbf{n}$ is the normal vector of the boundary. The resulting electric field leads to a linear band tilting in three dimensions and a logarithmic one in two dimensions, where the energy decreases from the negatively charged boundary to the positively charged boundary. When free charge carriers are present, which could be contributed by the substrate or could arise from defects in the ferroelectric material, the screening effect cancels the boundary charge, so that only the band bending near the boundary remains. In the following, we

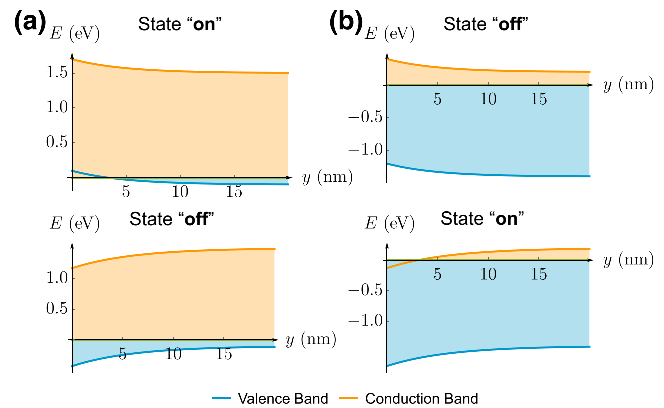

FIG. 1. A schematic of upward (top) and downward (bottom) band binding near the material edge, for a chemical potential (a) near the valence band and (b) near the conduction band. The Fermi energy of the electrode is set to be $E = 0$.

consider ferroelectric materials with a large band gap, so that the free charge carriers are from the metallic substrate. Due to the insufficient screening in two dimensions, the band bending can extend over quite a region (typically several nanometers) near the interface. For example, the scanning-tunneling-microscopy-measured band bending near the boundary of 1-ML SnTe film can be fitted nicely by an exponential function $V = \alpha e^{-y/\lambda} + c$ [25], which is sketched in Fig. 1. SnTe thin films with an odd number of monolayers all share similar band-bending profiles. We emphasize that this band bending near the interface generally exists for all ferroelectric thin films with in-plane polarization and does not depend crucially on material details.

III. DEVICE DESIGN

The robust band bending induced by in-plane polarization motivates us to propose a type of nonvolatile memory. The schematic of the device is shown in Fig. 2(a). The core of the design is a ferroelectric thin film sandwiched by a metallic substrate and a wide-band-gap insulator. The writing and reading electrodes are deposited at two different edges of the top insulator, which is (mostly) parallel to the polarization direction. In the figure, the in-plane polarization is assumed to be along the $+y$ direction, which will induce opposite net charges at different boundaries. Depending on the polarization direction ($+y$ or $-y$), the band bending near the reading electrode could be upward or downward, the mechanism for which has already been discussed in the previous paragraph. The band diagrams near one of the electrodes are shown in Figs. 2(b) and 2(c), where the chemical potential is set to be near the valence band.

To write the information or manipulate the polarization direction, one can apply a writing voltage $\pm V_W$ on the

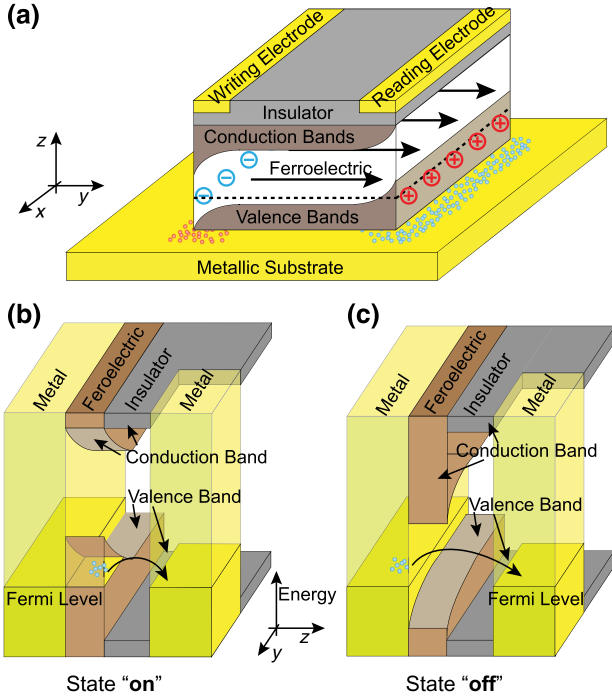

FIG. 2. A schematic of (a) the device and the band diagrams for the (b) "on" and (c) "off" sates. Here, the chemical potential is near the valence band, which corresponds to the left column in Fig. 1. The in-plane polarization induces bound charges and thus robust band bending around the boundary. Depending on the polarization direction, one of the edges could be (b) conducting or (c) insulating, which will change the effective potential barrier between the reading electrode and the substrate, therefore realizing bistable states with different tunneling currents. In (a), the large circles with "+/−" represent positive or negative bound charges induced by the ferroelectric polarization. The small red (blue) dots represent positive (negative) screening charges from the metallic substrate. The dashed line denotes the Fermi level.

writing electrode with reference to the reading electrode to generate an in-plane electric field across the ferroelectric thin film, thus forcing the polarization along the $\pm y$ direction regardless of the initial polarization direction. The stored information is represented by the $\pm y$ polarization direction, which can be seen as the "0/1" bit. The polarization persists for a longer duration even after the write voltage is turned off, and in this way the information storage is nonvolatile. The time cost of the writing operation is determined by the polarization switching time, which in turn is determined by the applied writing voltage V_W. For example, the coercive field in GeTe thin films is reported to be $E_c = 0.206$ V/nm, which translates to around $V_c = 20.6$ V for writing and reading electrodes separated by 100 nm [38]. For $V_W < V_c$, which is usually the case in a realistic device, the switching time is determined by the domain-wall dynamics and is typically several hundreds of picoseconds [39–41].

To read the information or measure the polarization direction, one can apply a reading voltage V_R on the reading electrode with reference to the metallic substrate and measure the tunneling current. The tunneling current depends on the band bending and hence the polarization direction. More specifically, if the chemical potential is near the valence or the conduction band, respectively, the charge carriers can be holes or electrons. In the case of hole charge carriers, the tunneling current in the "on" state I_{on}, where the band bends upward near the reading electrode, is significantly larger than that in the "off" state I_{off}, where the band bends downward. This is illustrated in Figs. 1(a)–1(c). In the case of electron charge carriers, the downward bending represents the "on" state and the upward bending represents the "off" state, as shown in Fig. 1(b). Since the electric field generated by the reading voltage is perpendicular to the polarization, the reading process is nondestructive. Note that no capacitor discharge is involved in this process: the time cost of the reading operation is almost solely determined by the peripheral-current-measurement device.

IV. THE TUNNELING CURRENT

We now turn to a detailed study of the tunneling-electroresistance effect between the metallic substrate and the reading electrode. Without loss of generality, we assume that the Fermi level of the metal is close to the valence band of the ferroelectric film. If the band bending is upward and sufficiently strong, the valence-band edge will be higher than the Fermi level of the metal, making the ferroelectric thin film conducting. In this case (the "on" state), the tunneling happens between the ferroelectric thin film and the reading electrode [Fig. 2(b)]. It is worth noting that the above discussion also works for the scenario of downward band bending if the Fermi level in the metal is close to the conduction band of the ferroelectric film and a parallel computation is presented in Ref. [42]. On the other hand (the "off" state), downward band bending makes the ferroelectric thin film insulating. The tunneling then happens between the metallic substrate and the reading electrode [Fig. 2(c)]. In this way, the threshold voltage for the "on" state is determined by the band gap and the thickness of the insulator, while the on:off ratio $I_{\text{on}}/I_{\text{off}}$ is determined by the band bending and the thickness of the ferroelectric thin film.

To make the above intuitive argument more concrete, we compute the tunneling current in a metal-ferroelectric-insulator-metal junction using the two-terminal Landauer formula:

$$I = \frac{2e}{h} \int_{-\infty}^{\infty} T(E)\,[f_L(E) - f_R(E)]\,dE = \frac{2e}{h} \int_0^U T(E) dE, \tag{1}$$

where $T(E)$ is the transmission probability and $f_{L/R}(E) = \left[e^{-(E-\mu_{L/R})/k_BT} + 1\right]^{-1}$ is the Fermi-Dirac distribution function. μ_L and μ_R are the chemical potentials of the left and the right electrodes, respectively. In the following, we always set $\mu_L = 0$ as the reference. At zero temperature, $f_{L/R}(E)$ becomes the step function and Eq. (1) reduces to its final form, where $U \equiv \mu_R - \mu_L$ is the voltage bias.

The geometry of the system is taken to be the same as the device design in Fig. 2, where from the $-z$ to $+z$ there are, in order, the left metal electrode (substrate), the ferroelectric, the insulator, and the right metal electrode (reading electrode). The dimensions are $X \times Y \times Z$. Here, $Z = d_{\mathrm{FE}} + d_I$, where d_{FE} and d_I are the thicknesses of the ferroelectric and the insulator film, respectively.

Inside the junction, the electrons and the holes are governed by the Schrödinger equation:

$$\left[-\frac{\hbar^2\nabla^2}{2m^*} + V(x,y,z)\right]\psi = E\psi. \tag{2}$$

The potential barrier of the ferroelectric $V(x,y,0 \le z < d_{\mathrm{FE}})$ is modeled by the fitted potential of 1-ML SnTe thin film [25,43]. The potential of the insulator $V(x,y,d_{\mathrm{FE}} \le z < d_{\mathrm{FE}} + d_I)$ is modeled by a square potential of monolayer hexagonal boron nitride [44]. All of the calculation details, including the parameters, can be found in Ref. [42].

Due to the complicated shape of the potential, the transmission probability in Eq. (1) is computed numerically using the Kwant software package [45], based on the discretized version given in Eq. (2). Both of the tunneling-current contributions from the electrons and the holes are taken into account. The results are summarized in Fig. 3. Since the magnitude of the tunneling current and the on:off ratio are two quantities that determine the sensitivity and the accuracy of the peripheral-current-measuring device, we mostly focus on them.

We first discuss the voltage-current characteristics [Fig. 3(a)]. When the reading voltage is very small, the current of the "on" state and that of the "off" state both come from the tunneling. With an increase in the voltage, there is first a threshold in the "on" state, after which $V > V_{\mathrm{on}}$ and Ohm's law $I \propto U$ governs. The threshold voltage of the "off" state V_{off} is larger than that of the "on" state. In Fig. 3(a), $V_{\mathrm{on}} \approx 0.1$ V and $V_{\mathrm{off}} \approx 0.4$ V. When the voltage is in between the two threshold voltages, i.e., $V_{\mathrm{on}} < V < V_{\mathrm{off}}$, a very large on:off ratio decreases exponentially with an increase in the voltage. In order to maximize the on:off ratio, it is important for the bias voltage to be within this "sweet spot."

From a device design point of view, the on:off ratio and the size of the "sweet spot" $V_{\mathrm{off}}/V_{\mathrm{on}}$ can be enhanced by increasing the d_{FE}/d_I ratio, as shown in Fig. 3(b). This can be understood from our intuitive argument before—the difference between the tunneling region of the "on" state and that of the "off" state is the ferroelectric film. This result

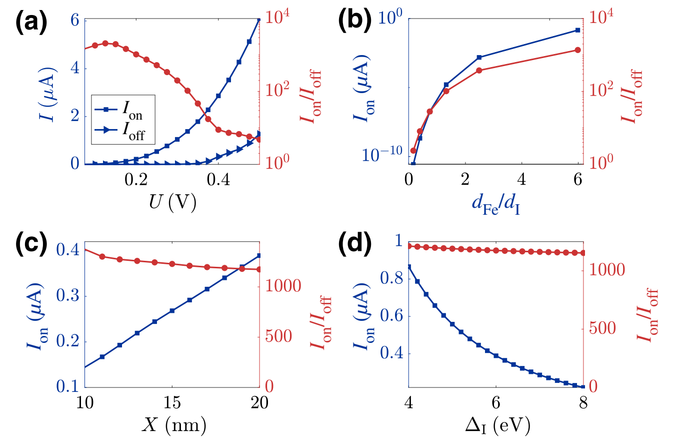

FIG. 3. The tunneling current computed from the Landauer formula [Eq. (1)] as a function of various parameters ($X = Y = 10$ nm, $d_{\mathrm{FE}} = 6$ nm, $d_I = 1$ nm, and $U = 0.18$ V if not specified): (a) the bias voltage U; (b) the ferroelectric:insulator thickness ratio d_{FE}/d_I (the total thickness is fixed at $Z = 7$ nm); (c) the device width X; (d) the insulator band gap Δ_I.

suggests that the thickness of the insulator film d_I should be small, but still large enough to prevent the electric discharge between the electrodes. Note that for a fixed total thickness, increasing d_{FE}/d_I also increases the magnitude of the "on"-state current significantly. The on:off ratio can be as large as about 1000 for $d_{\mathrm{FE}}/d_I = 6/1$.

The magnitude of the "on"-state current after the threshold $V > V_{\mathrm{on}}$ can be enhanced simply by increasing the width of the device in the x direction. As shown in Fig. 3(c), I_{on} increases linearly with X because the number of modes per unit energy in the electrode also grows linearly. It is also possible to increase the current magnitude by decreasing the band gap of the insulator layer Δ_I [Fig. 3(d)]. Note that for both approaches, the on:off ratio is almost unaffected, implying an independent control of the "on"-state current and the on:off ratio.

We emphasize that although Fig. 3 is computed using the parameter of SnTe, the qualitative conclusion is independent of the material. The device design and the transport model are completely general and are applicable to any nanoplates or even nanodots with in-plane ferroelectricity, where the band bending can be both upward or downward, located at the material edge or the ferroelectric-domain wall, and the charge carrier can be both electrons or holes.

V. CONCLUSION

In conclusion, we propose a type of ferroelectric memory based on in-plane polarization. Compared with the DRAM or the out-of-plane-polarization-based FERAM, our design has advantages including nonvolatility, a nondestructive reading operation, a faster reading and writing operation, and greater tunability of the tunneling current

and the on:off ratio. Our design is based on a ferroelectric thin film with an in-plane polarization component that is switchable by an external electric field. Compared with FTJs, in thin films the in-plane polarization is much more robust. The 2D nature of the material, i.e., the weak van der Waals interlayer coupling, makes the device easy to fabricate. In particular, boundary effects caused by lattice mismatching can be reduced greatly if the device is fabricated by stacking 2D materials [46,47].

A wide family of materials, for example, the IV-VI semiconductors XY, where $X = \mathrm{Ge,Sn,Pb}$ and $Y = \mathrm{S,Se,Te}$, along with their alloys (e.g., $Pb_xSn_{1-x}Te$ and $Pb_xSn_{1-x}Se$) and superlattices (e.g., PbTe/SnTe), are ideal candidates for the realization of our proposal [25,48–52]. Although SnTe nanoplates grown by molecular-beam epitaxy (MBE) are not scalable at the moment, we believe that as more 2D ferroelectrics are being discovered, 2D ferroelectrics that can grow with uniform crystalline orientations will soon be found. For example, it has already been found that In_2Se_3 has in-plane polarization and can be grown by both MBE and chemical-vapor deposition (CVD) [27–30]. We hope that our design can open up a new direction for ferroelectric nonvolatile memories.

ACKNOWLEDGMENTS

H.S. would like to thank Michal Papaj for helpful instructions on KWANT. This work is supported by the DOE Office of Basic Energy Sciences, Division of Materials Sciences and Engineering under Award de-sc0010526. J.L. acknowledges financial support from the Hong Kong Research Grants Council (Project No. ECS26302118). K.C. was funded by the Deutsche Forschungsgemeinschaft (DFG, German Research Foundation) Project Number PA 1812/2-1. L.F. is partly supported by the David and Lucile Packard Foundation.

[1] J. F. Scott, Multiferroic memories, Nat. Mater. **6**, 256 (2007).

[2] Kinam Kim and Dong Jin Jung, in *Ferroelectrics*, edited by Mickal Lallart (InTech, Rijeka, 2011), Chap. 6.

[3] Dudley Allen Buck, Ferroelectrics for Digital Information Storage and Switching, Type Tech. Rep. (Massachusetts Institute of Technology, 1952).

[4] James F. Scott and Carlos A. Paz de Araujo, Ferroelectric memories, Science **246**, 1400 (1989).

[5] James F. Scott, *Ferroelectric Memories* (Springer-Verlag, Berlin-Heidelberg, 2013), Vol. 3.

[6] J. T. Evans and R. Womack, An experimental 512-bit nonvolatile memory with ferroelectric storage cell, IEEE J. Solid State Circuits **23**, 1171 (1988).

[7] R. Womack and D. Tolsch, in *IEEE International Solid-State Circuits Conference, 1989 ISSCC. Digest of Technical Papers* (1989), p. 242.

[8] Hiroshi Ishiwara, Masanori Okuyama, and Yoshihiro Arimoto, *Ferroelectric Random Access Memories* (Springer-Verlag, Berlin-Heidelberg, 2004), Vol. 93.

[9] Shaoping Li, J. A. Eastman, Z. Li, C. M. Foster, R. E. Newnham, and L. E. Cross, Size effects in nanostructured ferroelectrics, Phys. Lett. A **212**, 341 (1996).

[10] Céline Lichtensteiger, Matthew Dawber, and Jean-Marc Triscone, *in Physics of Ferroelectrics: A Modern Perspective* (Springer-Verlag, Berlin-Heidelberg, 2007), p. 305.

[11] A. K. Tagantsev, I. Stolichnov, E. L. Colla, and N. Setter, Polarization fatigue in ferroelectric films: Basic experimental findings, phenomenological scenarios, and microscopic features, J. Appl. Phys. **90**, 1387 (2001).

[12] B. S. Kang, Jong-Gul Yoon, D. J. Kim, T. W. Noh, T. K. Song, Y. K. Lee, J. K. Lee, and Y. S. Park, Mechanisms for retention loss in ferroelectric $Pt/Pb(Zr_{0.4}Ti_{0.6})O_3/Pt$ capacitors, Appl. Phys. Lett. **82**, 2124 (2003).

[13] M. Ye Zhuravlev, R. F. Sabirianov, S. S. Jaswal, and E. Y. Tsymbal, Giant Electroresistance in Ferroelectric Tunnel Junctions, Phys. Rev. Lett. **94**, 246802 (2005).

[14] H. Kohlstedt, N. A. Pertsev, J. Rodríguez Contreras, and R. Waser, Theoretical current-voltage characteristics of ferroelectric tunnel junctions, Phys. Rev. B **72**, 125341 (2005).

[15] Evgeny Y. Tsymbal and Hermann Kohlstedt, Tunneling across a ferroelectric, Science **313**, 181 (2006).

[16] Dillon D. Fong, G. Brian Stephenson, Stephen K. Streiffer, Jeffrey A. Eastman, Orlando Auciello, Paul H. Fuoss, and Carol Thompson, Ferroelectricity in ultrathin perovskite films, Science **304**, 1650 (2004).

[17] D. D. Fong, A. M. Kolpak, J. A. Eastman, S. K. Streiffer, P. H. Fuoss, G. B. Stephenson, Carol Thompson, D. M. Kim, K. J. Choi, C. B. Eom, I. Grinberg, and A. M. Rappe, Stabilization of Monodomain Polarization in Ultrathin $PbTiO_3$ Films, Phys. Rev. Lett. **96**, 127601 (2006).

[18] D. A. Tenne, P. Turner, J. D. Schmidt, M. Biegalski, Y. L. Li, L. Q. Chen, A. Soukiassian, S. Trolier-McKinstry, D. G. Schlom, X. X. Xi, D. D. Fong, P. H. Fuoss, J. A. Eastman, G. B. Stephenson, C. Thompson, and S. K. Streiffer, Ferroelectricity in Ultrathin $BaTiO_3$ Films: Probing the Size Effect by Ultraviolet Raman Spectroscopy, Phys. Rev. Lett. **103**, 177601 (2009).

[19] Emad Almahmoud, Igor Kornev, and L. Bellaiche, Dependence of Curie temperature on the thickness of an ultrathin ferroelectric film, Phys. Rev. B **81**, 064105 (2010).

[20] K. S. Lee, J. H. Choi, J. Y. Lee, and S. Baik, Domain formation in epitaxial $Pb(Zr,Ti)O_3$ thin films, J. Appl. Phys **90**, 4095 (2001).

[21] Kui Yao, Bee Keen Gan, Meima Chen, and Santiranjan Shannigrahi, Large photo-induced voltage in a ferroelectric thin film with in-plane polarization, Appl. Phys. Lett **87**, 212906 (2005).

[22] S. Matzen, O. Nesterov, G. Rispens, J. A. Heuver, M. Biegalski, H. M. Christen, and B. Noheda, Super switching and control of in-plane ferroelectric nanodomains in strained thin films, Nat. Commun. **5**, 4415 (2014).

[23] Chuanshou Wang, Xiaoxing Ke, Jianjun Wang, Renrong Liang, Zhenlin Luo, Yu Tian, Di Yi, Qintong Zhang, Jing Wang, Xiu-Feng Han, Gustaaf Van Tendeloo, Long-Qing Chen, Ce-Wen Nan, Ramamoorthy Ramesh, and Jinxing Zhang, Ferroelastic switching in a layered-perovskite thin film, Nat. Commun. **7**, 10636 (2016).

[24] Kazuyuki Nakano, Masanori Ozaki, and Katsumi Yoshino, In-plane polarization reversal and boundary effect in transferred ferroelectric liquid crystal thin film, Jpn. J. Appl. Phys **41**, 5288 (2002).

[25] K. Chang, J. Liu, H. Lin, N. Wang, K. Zhao, Anmin Zhang, Feng Jin, Yong Zhong, Xiaopeng Hu, Wenhui Duan, Q. Zhang, L. Fu, Q.-K. Xue, X. Chen, and S.-H. Ji, Discovery of robust in-plane ferroelectricity in atomic-thick SnTe, Science **353**, 274 (2016).

[26] Kai Chang, Thaneshwor P. Kaloni, Haicheng Lin, Amilcar Bedoya-Pinto, Avanindra K. Pandeya, Ilya Kostanovskiy, Kun Zhao, Yong Zhong, Xiaopeng Hu, Qi-Kun Xue, Xi Chen, Shuai-Hua Ji, Salvador BarrazaLopez, and Stuart S. P. Parkin, Enhanced spontaneous polarization in ultrathin SnTe films with layered antipolar structure, Adv. Mater. **31**, 1804428 (2018).

[27] Wenjun Ding, Jianbao Zhu, Zhe Wang, Yanfei Gao, Di Xiao, Yi Gu, Zhenyu Zhang, and Wenguang Zhu, Prediction of intrinsic two-dimensional ferroelectrics in In_2Se_3 and other III_2-VI_3 van der Waals materials, Nat. Commun. **8**, 14956 (2017).

[28] Changxi Zheng, Lei Yu, Lin Zhu, James L. Collins, Dohyung Kim, Yaoding Lou, Chao Xu, Meng Li, Zheng Wei, Yupeng Zhang, Mark T. Edmonds, Shiqiang Li, Jan Seidel, Ye Zhu, Jefferson Zhe Liu, Wen-Xin Tang, and Michael S. Fuhrer, Room temperature in-plane ferroelectricity in van der Waals In_2Se_3, Sci. Adv. **4**, eaar7720 (2018).

[29] Chaojie Cui, Wei-Jin Hu, Xingxu Yan, Christopher Addiego, Wenpei Gao, Yao Wang, Zhe Wang, Linze Li, Yingchun Cheng, Peng Li, Xixiang Zhang, Husam N. Alshareef, Tom Wu, Wenguang Zhu, Xiaoqing Pan, and Lain-Jong Li, Intercorrelated in-plane and out-of-plane ferroelectricity in ultrathin two-dimensional layered semiconductor In_2Se_3, Nano Lett. **18**, 1253 (2018).

[30] Sock Mui Poh, Sherman Jun Rong Tan, Han Wang, Peng Song, Irfan H. Abidi, Xiaoxu Zhao, Jiadong Dan, Jingsheng Chen, Zhengtang Luo, Stephen J. Pennycook, Antonio H. Castro Neto, and Kian Ping Loh, Molecular-beam epitaxy of two-dimensional In_2S_3 and its giant electroresistance switching in ferroresistive memory junction, Nano Lett. **18**, 6340 (2018).

[31] R. R. Mehta, B. D. Silverman, and J. T. Jacobs, Depolarization fields in thin ferroelectric films, J. Appl. Phys. **44**, 3379 (1973).

[32] Javier Junquera and Philippe Ghosez, Critical thickness for ferroelectricity in perovskite ultrathin films, Nature **422**, 506 (2003).

[33] Zhongqing Wu, Ningdong Huang, Zhirong Liu, Jian Wu, Wenhui Duan, Bing-Lin Gu, and Xiao-Wen Zhang, Ferroelectricity in $Pb(Zr_{0.5}Ti_{0.5})O_3$ thin films: Critical thickness and 180° stripe domains, Phys. Rev. B **70**, 104108 (2004).

[34] Na Sai, Alexie M. Kolpak, and Andrew M. Rappe, Ferroelectricity in ultrathin perovskite films, Phys. Rev. B **72**, 020101 (2005).

[35] Na Sai, Craig J. Fennie, and Alexander A. Demkov, Absence of Critical Thickness in an Ultrathin Improper Ferroelectric Film, Phys. Rev. Lett. **102**, 107601 (2009).

[36] Yajun Zhang, Gui-Ping Li, Takahiro Shimada, Jie Wang, and Takayuki Kitamura, Disappearance of ferroelectric critical thickness in epitaxial ultrathin $BaZrO_3$ films, Phys. Rev. B **90**, 184107 (2014).

[37] J. A. Mundy, J. Schaab, Y. Kumagai, A. Cano, M. Stengel, I. P. Krug, D. M. Gottlob, H. Doğanay, M. E. Holtz, R. Held, Z. Yan, E. Bourret, C. M. Schneider, D. G. Schlom, D. A. Muller, R. Ramesh, N. A. Spaldin, and D. Meier, Functional electronic inversion layers at ferroelectric domain walls, Nat. Mater. **16**, 622 (2017).

[38] Wenhui Wan, Chang Liu, Wende Xiao, and Yugui Yao, Promising ferroelectricity in 2D group IV tellurides: A first-principles study, Appl. Phys. Lett. **111**, 132904 (2017).

[39] Rolf Landauer, Electrostatic considerations in $BaTiO_3$ domain formation during polarization reversal, J. Appl. Phys. **28**, 227 (1957).

[40] J. Li, B. Nagaraj, H. Liang, W. Cao, Chi H. Lee, and R. Ramesh, Ultrafast polarization switching in thin-film ferroelectrics, Appl. Phys. Lett. **84**, 1174 (2004).

[41] Kenjiro Fujimoto and Yasuo Cho, Nanosecond switching of nanoscale ferroelectric domains in congruent single-crystal $LiTaO_3$ using scanning nonlinear dielectric microscopy, Jpn. J. Appl. Phys. **43**, 2818 (2004).

[42] See the Supplemental Material at http://link.aps.org/supplemental/10.1103/PhysRevApplied.11.024048 for the calculation details.

[43] O. Madelung, U. Rössler, and M. Schulz, eds., in *Non-Tetrahedrally Bonded Elements and Binary Compounds I* (Springer-Verlag, Berlin-Heidelberg, 1998), p. 1.

[44] Yoichi Kubota, Kenji Watanabe, Osamu Tsuda, and Takashi Taniguchi, Deep ultraviolet light-emitting hexagonal boron nitride synthesized at atmospheric pressure, Science **317**, 932 (2007).

[45] Christoph W. Groth, Michael Wimmer, Anton R. Akhmerov, and Xavier Waintal, Kwant: A software package for quantum transport, New J. Phys. **16**, 063065 (2014).

[46] Joel I. Jan Wang, Yafang Yang, Yu-An Chen, Kenji Watanabe, Takashi Taniguchi, Hugh O. H. Churchill, and Pablo Jarillo-Herrero, Electronic transport of encapsulated graphene and WSe_2 devices fabricated by pick-up of prepatterned hBN, Nano Lett. **15**, 1898 (2015).

[47] Zaiyao Fei, Wenjin Zhao, Tauno A. Palomaki, Bosong Sun, Moira K. Miller, Zhiying Zhao, Jiaqiang Yan, Xiaodong Xu, and David H. Cobden, Ferroelectric switching of a two-dimensional metal, Nature **560**, 336 (2018).

[48] Hua Wang and Xiaofeng Qian, Two-dimensional multiferroics in monolayer group IV monochalcogenides, 2D Mater. **4**, 015042 (2017).

[49] Menghao Wu and Xiao Cheng Zeng, Intrinsic ferroelasticity and/or multiferroicity in two-dimensional phosphorene and phosphorene analogues, Nano Lett. **16**, 3236 (2016).

[50] Kai Liu, Jinlian Lu, Silvia Picozzi, Laurent Bellaiche, and Hongjun Xiang, Intrinsic Origin of Enhancement of Ferroelectricity in SnTe Ultrathin Films, Phys. Rev. Lett. **121**, 027601 (2018).

[51] Paul Z. Hanakata, Alexandra Carvalho, David K. Campbell, and Harold S. Park, Polarization and valley switching in monolayer group-IV monochalcogenides, Phys. Rev. B **94**, 035304 (2016).

[52] Mehrshad Mehboudi, Benjamin M. Fregoso, Yurong Yang, Wenjuan Zhu, Arend van der Zande, Jaime Ferrer, L. Bellaiche, Pradeep Kumar, and Salvador Barraza-Lopez, Structural Phase Transition and Material Properties of Few-Layer Monochalcogenides, Phys. Rev. Lett. **117**, 246802 (2016).